J. Fluid Mech. (2005), vol. 536, pp. 347–366.
doi:10.1017/S002211200500491X Printed in the United Kingdom

Nonlinear distortion of travelling waves in variable-area ducts with base flow: a quasi-one-dimensional analysis

By MANAV TYAGI[1] AND R. I. SUJITH[2]†

[1]Department of Mechanical Engineering, Indian Institute of Technology, Madras, Chennai 600036, India

[2]Department of Aerospace Engineering, Indian Institute of Technology Madras, Chennai 600036, India

(Received 12 November 2003 and in revised form 24 February 2005)

This paper presents an investigation of the nonlinear steepening of a gasdynamic disturbance propagating in a steady non-uniform base flow. The base flow is the steady compressible flow of a gas in a variable-area duct. The quasi-one-dimensional continuity, momentum and energy equations for the unsteady disturbance in homentropic flow are solved using the method of characteristics (wave front expansion technique). A closed-form solution for the slope of the disturbance at the wave front is obtained. The solution admits singularity for a compressive disturbance, which is responsible for the formation of shock in the flow. The solution is general and is applicable in any range of Mach number of the base flow. A special case of the steady gas flow in a convergent–divergent duct (C-D nozzle), where the flow makes a transition from subsonic to supersonic and vice versa, is investigated.

1. Introduction

The problem of shock formation in various flow situations is of great practical interest and has been studied for a long time. A shock arises owing to the nonlinear distortion of a finite-amplitude disturbance. The classical problem of the steepening of a plane wave into a shock in a constant-area duct with homentropic flow can be found in many text books of gasdynamics. In this simple case, the Riemann invariants are constant along the characteristics and thus it is possible to find an exact solution for the one-dimensional gas dynamics equations using the method of characteristics (Courant & Friedrichs 1948; Liepmann & Roshko 1957). The solutions so obtained become multi-valued in finite time. Since multi-valued solutions are impossible, a shock (jump) is formed at that location. It can also be shown that in the case of an ideal gas, only compressive disturbances can steepen into shock, whereas the expansive disturbances relax.

However, this classical treatment of shock formation is limited only to plane-wave propagation in a constant-area duct with homentropic flow. The propagation of plane waves in variable-area ducts with non-uniform flow is quite complex. In this case, the Riemann invariants are no longer constant along the characteristics and an exact solution of the problem is yet to be found. An important example of shock formation in a variable-area duct with non-uniform flow is shock formation in converging–diverging flow passages in rocket or jet engine nozzles and in intakes (diffusers) of

† Author to whom correspondence should be addressed. sujith@iitm.ac.in

supersonic vehicles. In a rocket nozzle, the flow accelerates from a subsonic region (after combustion) to a supersonic region. The source of disturbance could be the unsteady combustion, taking place in the combustor. Such a disturbance will propagate along the accelerating flow. In the air intake of a supersonic vehicle, for example, air-breathing engines (turbojet/ramjet/scramjet), steady shocks are present in the front part of the vehicle. Owing to a sudden variation in the speed of vehicle or change in ambient conditions, these steady shocks fluctuate and cause the disturbances to propagate along the decelerating flow. Therefore, determination of shock formation in a convergent–divergent nozzle is an important problem, and a detailed analysis of such a problem could be useful for the design of nozzles and intakes in supersonic vehicles.

Since shock is formed owing to the inertial overtaking of flow particles, shock formation in a flow could be related to its inertial stability. If in a given gasdynamic flow, shock formation is favoured, the flow is inertially unstable towards a gasdynamic disturbance and if shock formation is opposed, the flow is inertially stable towards a gasdynamic disturbance. In fact, the stability of accelerating and decelerating flow in the transonic region in a convergent–divergent (C-D) nozzle has been a concern for a long time. Kantrowitz (1947) made the first attempt to understand the stability of quasi-one-dimensional steady transonic flow. He concluded that an accelerating transonic flow is stable and a decelerating transonic flow is unstable. Kuo (1951) investigated the stability of a triangular pulse in transonic flow by solving the potential flow equation for unsteady two-dimensional flow. His analysis showed that accelerating transonic flow is stable for an unsteady disturbance over a convex surface (aerofoil). On the other hand, decelerating transonic flow is unstable for a compression pulse over a convex surface. Prasad published a series of papers concerning the stability of transonic flow. He derived a nonlinear approximate equation for a hyperbolic system and studied the stability of two-dimensional steady spiral flow of compressible fluid (Prasad 1972). He showed that the flow is unstable if the sonic transition occurs from a supersonic state to a subsonic state and it is stable when the transition is from a subsonic state to a supersonic state. A similar analysis was performed in Prasad (1973). Prasad & Krishnan (1977) considered wave propagation in a two-dimensional steady transonic flow and investigated the turning effect of a wave front. Prasad (2001) explained the BKPS (Bhatnagar, Kulikovskii, Prasad and Slobodkina) theory, which was initially developed by Kulikovskii & Slobodkina (1967) and was further extended by Bhatnagar & Prasad (1971). This theory is essentially based on the method of phase plane for a nonlinear system. Using this theory he explained (in a quasi-one-dimensional flow in a C-D nozzle) why an accelerating transonic flow is stable and why it is difficult to obtain stable decelerating transonic flow experimentally.

Although there has been much work on the stability of flow in C-D nozzles, the questions of whether a disturbance will steepen into a shock or not and where the location of the shock will be have not been answered in the literature. The present paper gives a detailed analytical treatment of the nonlinear steepening of a disturbance in a variable-area duct with steady non-uniform base flow, with an example of flow in a C-D nozzle. The flow is assumed to be quasi-one-dimensional. Therefore, the two-dimensional and wave front turning effects are not taken into account. However, the present analysis is much simpler and gives the detailed analysis of wave front steepening in C–D nozzles. The main results of the work are to give the condition of shock formation and the corresponding location of the shock.

As mentioned in the beginning of this section, the Riemann invariants are not constant along the characteristics in a non-uniform flow. However, if we consider that the disturbance comprises of the wave with a discontinuous first derivative at the wave front (Whitham 1974), it is possible to find a global solution in closed form, at least for the slope of the dependent variables at the wave front. The location and time of shock formation can then easily be obtained as they are singular points of the solution. This technique is called ‘wave front expansion’. Any disturbance produced in finite time (for example by a moving piston) in a diffusion-free medium will have a discontinuity in the first derivative of the flow variable (slope), but not in the value of the flow variable (amplitude). Therefore, for the existence of such a disturbance, it is assumed that the propagation of the disturbance is purely hyperbolic.

Lin & Szeri (2001) used the wave front expansion technique to study the nonlinear steepening of plane and spherical wave fronts in the presence of an entropy gradient. They found that shock formation is favoured by negative entropy gradients and is opposed by positive entropy gradients. Tyagi & Sujith (2003) applied the same technique to investigate the effect of area variation and entropy gradients on shock formation in a quiescent flow. Their analysis showed that the shock formation distance is shorter in converging ducts and longer in diverging ducts as compared to that of a constant-area duct. Tyagi & Sujith (2003) considered wave propagation in a quiescent flow. In the present paper, we extend this analysis to the case of wave propagation in a variable-area duct with an initially present steady non-uniform flow. This initially present steady non-uniform flow in the variable-area duct will be referred to as ‘base flow’ in the rest of the paper.

The paper is organized as follows. The evolution equation for the first derivative of particle velocity at the wave front is derived in § 2 and solved in § 3. Sections 4 and 5 give the detailed analyses of right- and left-running waves in non-uniform flow (flow in convergent–divergent nozzles). Finally, § 6 draws conclusions.

2. Evolution equation for the first derivative of particle velocity at the wave front

In this section, an evolution equation is derived for the first derivative of particle velocity at the wave front. The quasi-one-dimensional continuity and momentum equations for an inviscid gas can be written as (Thompson 1972)

Continuity:

$$\frac{\partial \rho}{\partial t} + \rho \frac{\partial u}{\partial x} + u \frac{\partial \rho}{\partial x} + \frac{\rho u}{A}\frac{\mathrm{d}A}{\mathrm{d}x} = 0, \tag{2.1}$$

Momentum:

$$\frac{\partial u}{\partial t} + u \frac{\partial u}{\partial x} + \frac{1}{\rho}\frac{\partial p}{\partial x} = 0. \tag{2.2}$$

In a homentropic flow, for an ideal gas, pressure and density are related by the following relation:

$$p = k\rho^{\gamma}, \tag{2.3}$$

where γ is the ratio of specific heats of the gas and k is a function of the reference pressure and reference density. Equations (2.1) and (2.2) form a hyperbolic system having characteristic velocities $u + a$ and $u - a$ (Courant & Friedrichs 1948), where $a(=\sqrt{\gamma p/\rho})$ is the speed of sound. Following the derivation of Lin & Szeri (2001) or Tyagi & Sujith (2003), (2.1) and (2.2) can be recast as:

$$A\frac{\partial a}{\partial t} + Au\frac{\partial a}{\partial x} + \frac{\gamma - 1}{2}Aa\frac{\partial u}{\partial x} + \frac{\gamma - 1}{2}ua\frac{\mathrm{d}A}{\mathrm{d}x} = 0, \tag{2.4}$$

$$\frac{\partial u}{\partial t} + u\frac{\partial u}{\partial x} + \frac{2}{\gamma - 1}a\frac{\partial a}{\partial x} = 0. \tag{2.5}$$

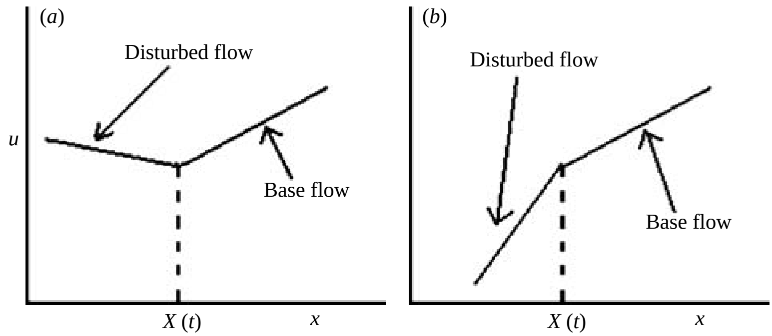

FIGURE 1. The effect of a right-running disturbance on the base flow. (*a*) Compression wave increases the velocity of base flow at the wave front. (*b*) Expansion wave decreases the velocity of base flow at the wave front.

In order to study the behaviour of a wave front, the wave front expansion technique will be applied (Whitham 1974). A detailed explanation of this technique can be found in Tyagi & Sujith (2003). In this technique, it is assumed that the wave at the wave front is discontinuous in its first derivative, i.e. dependent variables such as velocity, pressure and density of the gas have a discontinuous first derivative at the leading edge of the wave.

The evolution of a right-running wave front is considered first. Let the position of the wave front after time t be $x = X(t)$. The velocity of a right-running wave front will be

$$\frac{\mathrm{d}x}{\mathrm{d}t} = \dot{X}(t) = [u + a]_{x=X(t)}. \tag{2.6}$$

While performing the wave front expansion, the frame of reference is fixed to the moving wave front. In this frame of reference, the position of a particle will be $\xi = x - X(t)$. Downstream of the wave front, i.e. for $\xi > 0$, there is an undisturbed steady base flow. Upstream of the wave front, i.e. for $\xi < 0$, the flow is unsteady. Figure 1 shows the compression and expansion of a given steady base flow by a right-running wave. Expanding the dependent variables as a Taylor series about the wave front gives:

$$\left.\begin{aligned} a(X(t)+\xi,t) &= a_0(X(t)) + \xi a_0'(X(t)) + \tfrac{1}{2}\xi^2 a_0''(X(t)) + \cdots \\ u(X(t)+\xi,t) &= u_0(X(t)) + \xi u_0'(X(t)) + \tfrac{1}{2}\xi^2 u_0''(X(t)) + \cdots \\ A(X(t)+\xi) &= A(X(t)) + \xi A'(X(t)) + \tfrac{1}{2}\xi^2 A''(X(t)) + \cdots \end{aligned}\right\} \quad \xi > 0, \tag{2.7a}$$

$$\left.\begin{aligned} a(X(t)+\xi,t) &= a_0(X(t)) + \xi a_1(t) + \tfrac{1}{2}\xi^2 a_2(t) + \cdots \\ u(X(t)+\xi,t) &= u_0(X(t)) + \xi u_1(t) + \tfrac{1}{2}\xi^2 u_2(t) + \cdots \\ A(X(t)+\xi) &= A(X(t)) + \xi A'(X(t)) + \tfrac{1}{2}\xi^2 A''(X(t)) + \cdots \end{aligned}\right\} \quad \xi < 0. \tag{2.7b}$$

Note that $u_0(x)$, $a_0(x)$ and $A(x)$ are the velocity of the base flow, the speed of sound and the cross-sectional area of the duct, respectively. In fact, for a homentropic steady flow, the cross-sectional area of the duct $A(x)$ specifies $u_0(x)$ and $a_0(x)$. Using (2.6), the velocity of the wave front becomes $\dot{X}(t) = a_0(X(t)) + u_0(X(t))$. The expansions in (2.7) are substituted into (2.4) and (2.5) and the coefficients of ξ^0, ξ^1 are equated. After performing the required manipulations, we obtain the following evolution equation for $u_1(t)$:

$$\frac{\mathrm{d}u_1}{\mathrm{d}t} + p + qu_1 + ru_1^2 = 0, \tag{2.8}$$

where

$$\begin{aligned}
p &= \frac{1}{2}\left(-\frac{u_0''\dot{X}(t)^2}{a_0} + \frac{u_0'a_0'\dot{X}(t)^2}{a_0^2} - \frac{u_0'\ddot{X}(t)}{a_0} + \frac{u_0'\dot{X}(t)A'}{A} - \frac{(\gamma-1)u_0u_0'\dot{X}(t)A'}{2a_0A} \right. \\
&\quad \left. + \frac{(\gamma-1)u_0'^2\dot{X}(t)^2}{2a_0^2} + \frac{2a_0'\dot{X}(t)A'}{(\gamma-1)A} + \frac{u_0a_0A''}{A} \right), \\
q &= \frac{1}{2}\left(\frac{(\gamma-1)u_0A'}{2A} + \frac{a_0A'}{A} - \frac{(3\gamma-1)u_0'\dot{X}(t)}{2a_0} \right), \\
r &= \tfrac{1}{2}(\gamma+1).
\end{aligned}$$

The base flow is governed by the following gasdynamic equations (John 1984):

$$a_0^2 + \tfrac{1}{2}(\gamma-1)u_0^2 = a_{0s}^2, \tag{2.9a}$$

$$u_0'\left(1 - \frac{u_0^2}{a_0^2}\right) = -\frac{u_0A'}{A}, \tag{2.9b}$$

where a_{0s} is the stagnation speed of sound.

Equation (2.8) is the generalized Riccati equation. Since p, q and r are functions of the variable $X(t)$, it is convenient to use $X(t)$ rather than t as an independent variable. Using

$$\frac{\mathrm{d}u_1}{\mathrm{d}t} = \frac{\mathrm{d}u_1}{\mathrm{d}X(t)}\frac{\mathrm{d}X(t)}{\mathrm{d}t} = \frac{\mathrm{d}u_1}{\mathrm{d}y}\dot{X}(t),$$

where $y = X(t)$ and $\dot{X}(t) = a_0(y) + u_0(y)$, (2.8) becomes

$$\frac{\mathrm{d}u_1}{\mathrm{d}y} + P + Qu_1 + Ru_1^2 = 0. \tag{2.10}$$

Here $P = p/\dot{X}(t)$, $Q = q/\dot{X}(t)$ and $R = r/\dot{X}(t)$. Thus, P, Q and R are known functions of y for a given duct having a steady base flow. Equation (2.10) governs the evolution of the first derivative of the particle velocity at the wave front, $u_1(y)$ as a function of the location of wave front (y). When there is no disturbance, the first derivative of the particle velocity is $u_0'(y)$, i.e. the same as the first derivative of steady base flow velocity. In the present analysis, at some location (say $y = 0$), this is changed from $u_0'(0)$ to $u_1(0)$ owing to some disturbance. This introduces a discontinuity in the first derivative of particle velocity at the wave front that propagates along the characteristics at the characteristic velocity $\dot{X}(t)$.

3. Solution of Riccati's equation

In general, it is not possible to integrate Riccati's equation (2.10) for u_1. However, Riccati's equation can be reduced to a linear first-order ordinary differential equation if a particular integral is known (Davis 1962). In the absence of any disturbance, the first derivative of the particle velocity at the wave front remains constant at all times and is equal to the first derivative of the particle velocity in the steady base flow. Therefore $u_0'(y)$ is a particular integral of (2.10). This can easily be justified by substituting $u_1 = u_0'$ in the right-hand side of (2.10), which gives

$$\frac{\mathrm{d}u_0'}{\mathrm{d}y} + P + Qu_0' + Ru_0'^2 = 0. \tag{3.1}$$

This relation can be used to eliminate P from (2.10). For this purpose, u_1 is written as a sum of u_0' and some function $\sigma(y)$, and then substituted into (2.10). Using (3.1), the resultant equation simplifies to

$$\frac{\mathrm{d}\sigma}{\mathrm{d}y} + (Q + 2u_0'R)\sigma + R\sigma^2 = 0. \tag{3.2}$$

Indeed, the above mathematical trick clears the physics of the propagation of the wave front in a non-uniform steady flow (base flow). The variable u_1, the first derivative of particle velocity at the wave front, contains contributions, both from the base flow and the unsteady disturbance. In the base flow, the first derivative of particle velocity is $u_0'(y)$ which is governed by the relation (3.1). The function $\sigma(y)$ can then be thought of as the contribution from the unsteady disturbance to u_1 whose evolution is governed by (3.2). In fact, we may think of $\sigma(y)$ as the equivalent 'slope of the unsteady disturbance at the wave front'. In the rest of the paper, $\sigma(y)$ will be referred as the *slope of the disturbance*. The term $\sigma(y)$ is negative for compression waves and positive for expansion waves.

Equation (3.2) is similar to the equations derived by Lin & Szeri (2001) and Tyagi & Sujith (2003). In (3.2), the coefficient of the nonlinear term R is responsible for the nonlinear steepening of the wave front. Since R is always positive, the nonlinear term will try to decrease the value of σ. Thus, the nonlinear term makes a negative value of σ more negative and a positive value of σ less positive. Thus, the nonlinearity alone causes a compression wave front to steepen and an expansion wave front to relax. The linear term $(Q + 2u_0'R)\sigma$ in (3.2) is due to the non-uniform medium. It takes into account the gradient in the flow variables as well as the geometrical changes due to the area variation. The linear term has the same effect on both compression and expansion wave fronts. If we neglect the effect of the nonlinear term, it is clear that the magnitude of σ will decrease when $(Q + 2u_0'R)$ is positive and increase when $(Q + 2u_0'R)$ is negative.

The solution of (3.2) (see Tyagi & Sujith 2003) is

$$\frac{1}{\sigma(y)} = \frac{IF(0)}{IF(y)\sigma(0)} + \frac{1}{IF(y)}\int_0^y IF(y)R(y)\,\mathrm{d}y, \tag{3.3}$$

where the integrating factor is

$$IF = \exp\left(-\int (Q + 2Ru_0')\,\mathrm{d}y\right). \tag{3.4}$$

Using (2.9), Q and R can be written as

$$Q(y) = \frac{1}{2}\left(-\frac{u_0'}{u_0} - \left(\frac{\gamma-1}{2}\right)\frac{4u_0'}{a_0} + \left(\frac{\gamma-1}{2}\right)\frac{u_0u_0'}{a_0^2}\right), \tag{3.5a}$$

$$R(y) = \frac{(\gamma+1)}{2(a_0+u_0)}. \tag{3.5b}$$

Performing the required integration, the integrating factor can be expressed as

$$IF(y) = \frac{2a_0\left(1 + \frac{1}{2}(\gamma-1)M^2\right)\sqrt{M}}{(\gamma-1)(M+1)^2}. \tag{3.6}$$

Here, $M = u_0/a_0$ is the Mach number of the base flow.

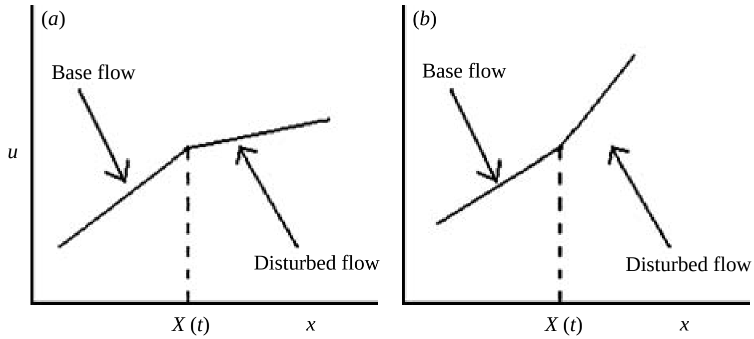

FIGURE 2. The effect of a left-running disturbance on the base flow. (*a*) Compression wave decreases the velocity of base flow at the wave front. (*b*) Expansion wave increases the velocity of base flow at the wave front.

Similarly, for a left-running wave front, the integrating factor can be expressed as:

$$IF(y) = \frac{2a_0\left(1+\frac{1}{2}(\gamma-1)M^2\right)\sqrt{M}}{(\gamma-1)(M-1)^2} \tag{3.7}$$

Figure 2 shows the compression and expansion of a given steady base flow by a left-running wave.

4. Nonlinear steepening of a right-running wave

This section investigates the steepening of a right-running wave front into a shock. Since the base flow velocity $u_0(y)$ and its derivative $u_0'(y)$ are finite, shock will form when $\sigma(y)$ becomes infinite. This occurs when the right-hand side of (3.3) vanishes. Since $IF(y) > 0$, shock can form only when $\sigma(0) < 0$, i.e. the initial disturbance is compressive. If it is assumed that the base flow field is extended up to infinity, the condition for shock formation can be obtained as:

$$|\sigma(0)| > \frac{IF(0)}{\displaystyle\int_0^\infty IF(y)R(y)\,\mathrm{d}y}. \tag{4.1}$$

Here, $|\sigma(0)|$ is the magnitude of $\sigma(0)$. The location of shock, y^* is given by:

$$\int_0^{y^*} IF(y)R(y)\,\mathrm{d}y = \frac{IF(0)}{|\sigma(0)|}. \tag{4.2}$$

4.1. *An example of flow in a converging–diverging* (*C-D*) *nozzle*

The above analysis can be used to study the steepening of a unsteady disturbance generated in a choked C-D nozzle, where the flow transits from subsonic to supersonic and vice versa (John 1984). The homentropic steady flow in a C-D nozzle is chosen as the base flow. The base flow considered here is such that Mach number is either an increasing or decreasing function along the nozzle (it is assumed that there is no steady shock in the diverging part of the nozzle). The origin of the coordinate system ($x = 0$) is fixed at the throat of nozzle. It is assumed that the nozzle is extended from $-\infty$ to $+\infty$ (a finite nozzle always forms a part of such an infinitely large nozzle). Therefore, when the Mach number of the base flow increases along the nozzle (accelerating flow), its value at the left-hand extreme end ($-\infty$) is zero and becomes infinite at the right-hand extreme ($+\infty$). The reverse of this occurs when the Mach number of the base flow decreases along the nozzle (decelerating flow). For a choked flow in a C-D nozzle, the Mach number $M(x)$ and cross-sectional area of the nozzle are related by the following relation (John 1984):

$$\frac{A(x)}{A(0)} = \frac{1}{M(x)}\left(\frac{\frac{1}{2}(\gamma+1)}{1+\frac{1}{2}(\gamma-1)M(x)^2}\right)^{(\gamma+1)/(2-2\gamma)}, \tag{4.3}$$

where$A(0)$ is the cross-sectional area at the throat of the C-D nozzle.

Consider a right-running wave front that starts at the location $x = x_i$ ($y = 0$ and $t = 0$) in the nozzle. The expressions for the location of shock (4.2) and the condition of shock formation (4.1) can be written in the following form:

$$\int_0^{y^*} \frac{f(M)}{f(M_i)}\mathrm{d}y = \frac{2a_{0i}(M_i+1)}{(\gamma+1)|\sigma_i|} = \beta_i, \tag{4.4}$$

$$|\sigma_i| > \frac{2a_{0i}(M_i+1)}{(\gamma+1)\displaystyle\int_0^{\infty}\frac{f(M)}{f(M_i)}\,\mathrm{d}y}. \tag{4.5}$$

Where the function $f(M)$ is:

$$f(M) = \frac{IF(y)}{a_0+u_0} = \frac{2\left(1+\frac{1}{2}(\gamma-1)M^2\right)\sqrt{M}}{(\gamma-1)(M+1)^3}. \tag{4.6}$$

The value of the variables at $x = x_i$ is identified by the subscript i. β_i is the shock formation distance in a constant-area duct having a uniform base flow at a Mach number M_i. The static speed of sound a_{0i} is related to the stagnation one as:

$$a_{0i} = \frac{a_{0s}}{\sqrt{1+\frac{1}{2}(\gamma-1)M_i^2}}. \tag{4.7}$$

Using (4.7), we can write β_i as:

$$\beta_i = \beta_s\frac{1+M_i}{\sqrt{1+\frac{1}{2}(\gamma-1)M_i}}, \tag{4.8}$$

where $\beta_s = 2a_{0s}/((\gamma+1)|\sigma_i|)$ is the shock formation distance in a constant-area duct in the stagnant condition. Thus, β_i is a function of the Mach number and is always greater than β_s.

Physically, the function $f(M)$ tells us about the effect of non-uniform flow on wave steepening. In the present paper, the properties of this function will be exploited to explain the physics of wave steepening in subsonic and supersonic flows (in a C-D nozzle). In order to perform this analysis, we must choose some reference with which the shock formation in a general non-uniform flow can be compared. In the present paper, the shock formation distance will be compared with β_i. This makes the analysis simpler and provides insight into the physics of the problem. If y^* is less than β_i, shock formation is favoured and if y^* is greater than β_i, shock formation is opposed. Such comparisons give the overall tendency of a wave front to form a shock. During the propagation of disturbance (before shock formation), the slope of the disturbance ($\sigma(y)$) might increase or decrease at different points. However, the present analysis compares the net effect of non-inform flow on the shock formation distance. Using (4.4), we can then write that shock formation is favoured if:

$$y^* < \beta_i \Rightarrow y^* < \int_0^{y^*}\frac{f(M)}{f(M_i)}\,\mathrm{d}y$$

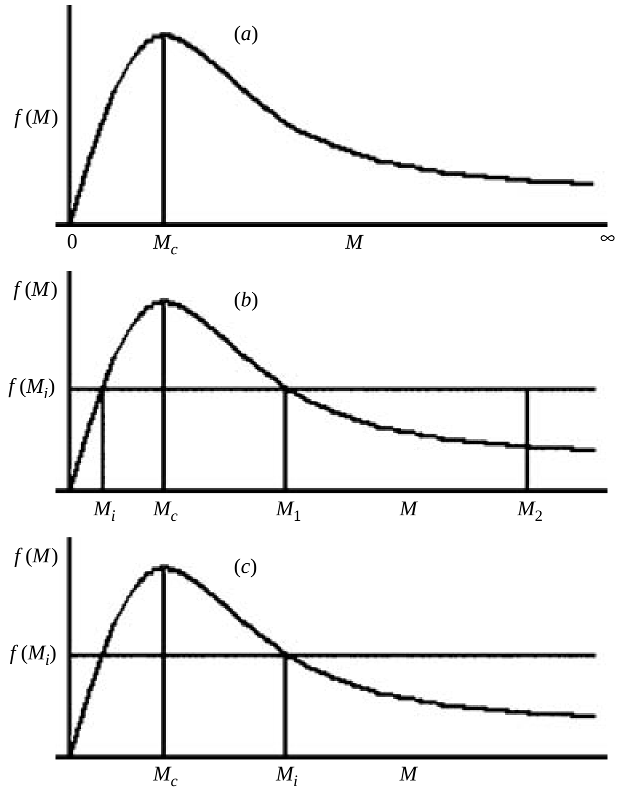

FIGURE 3. (a) Plot of $f(M)$ as function of M. The function $f(M)$ attains maximum value at $M = M_c$. (b) The case when the disturbance is created before M_c. (c) The case when the disturbance is created after M_c.

or

$$\int_0^{y^*} \frac{f(M) - f(M_i)}{f(M_i)}\, \mathrm{d}y > 0, \tag{4.9}$$

and shock formation is opposed if:

$$y^* > \beta_i \Rightarrow y^* > \int_0^{y^*} \frac{f(M)}{f(M_i)}\, \mathrm{d}y$$

or

$$\int_0^{y^*} \frac{f(M) - f(M_i)}{f(M_i)}\, \mathrm{d}y < 0. \tag{4.10}$$

The integral $\int_0^{y^*} (f(M) - f(M_i))/f(M_i)\, \mathrm{d}y$ is merely the difference $\beta_i - y^*$.

4.1.1. *Accelerating flow*

In an accelerating base flow in a C-D nozzle, the Mach number $M = M(x)$ is an increasing function, and thus has a one-to-one correspondence with the distance x. Therefore instead of x, M can be treated as the independent variable along the nozzle length. The plot of $f(M)$ versus M for $\gamma = 1.4$ is shown in figure 3(a). The maximum value of $f(M)$ occurs at a point M_c. Therefore, M_c will be a root of the equation,

$$f'(M_c) = 0. \tag{4.11}$$

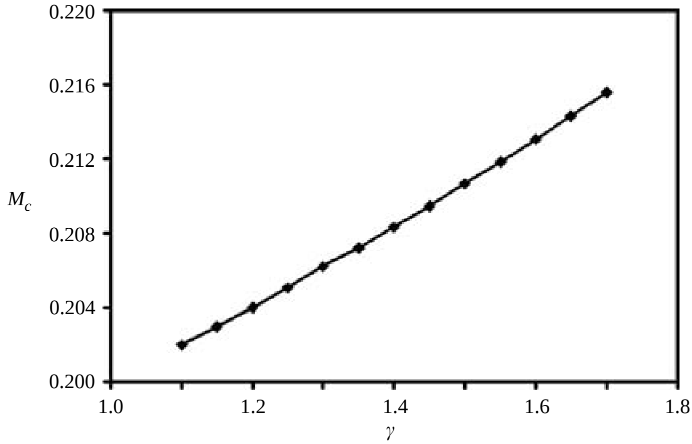

FIGURE 4. Plot of M_c as a function of γ.

Using (4.6), we obtain the following cubic equation for M_c:

$$(\gamma-1)M_c^3 - 5(\gamma-1)M_c^2 + 10M_c - 2 = 0. \tag{4.12}$$

Equation (4.12) can be solved explicitly for M_c. Introducing the number†

$$\delta = \gamma - 1, \tag{4.13}$$

and

$$B = \left[\left(-198 + 125\delta + 3\sqrt{\frac{6}{\delta}}\sqrt{125\delta^2 - 524\delta + 500}\right)\delta^2\right]^{1/3}, \tag{4.14}$$

then

$$M_c = \frac{B + 5\delta}{3\delta} + \frac{25\delta - 30}{3B}. \tag{4.15}$$

The following series expansion in the powers of δ can be used to calculate M_c, which exploits the smallness of δ:

$$M_c = 0.2 + 0.0192\delta + 0.003696\delta^2 + 0.00084080640\delta^3 + \cdots. \tag{4.16}$$

The first two terms of the above series give a sufficiently accurate value of M_c. The plot of M_c as a function of γ is shown in figure 4. It should be noted that M_c is a property of gas (depending only on γ).

The Mach number M_i can take any positive value i.e. the disturbance can start at any point in the nozzle. However, there are some interesting differences in the two cases, one in which the disturbance starts before M_c $(M_i < M_c)$ and the other in which the disturbance starts after M_c $(M_i > M_c)$.

Case 1

Figure 3(b) depicts the case when M_i is less than M_c. It is clear that $f(M_i)$ intersects the curve $f(M)$ at the two points M_i and M_1. From M_i to M_1, (4.9) holds and consequently shock formation is favoured. At the point y_1 (corresponding to the Mach number M_1), the integral $\int_0^y (f(M) - f(M_i))/f(M_i)\,\mathrm{d}y$ attains its maximum

† The authors are grateful to an anonymous referee for providing the exact explicit solution of equation (4.12).

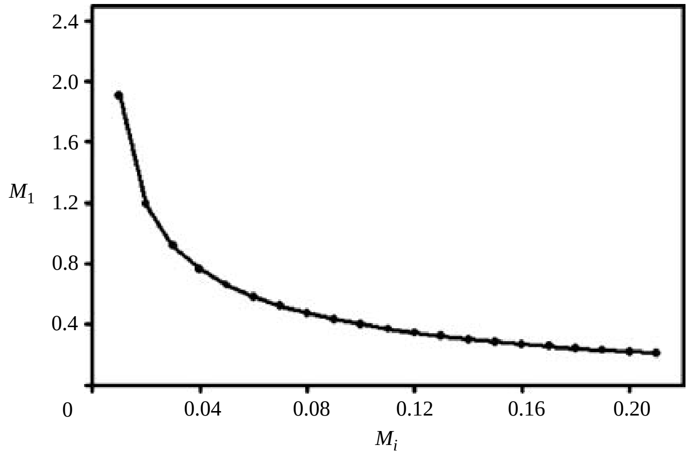

FIGURE 5. Plot of M_1 as a function of M_i for $\gamma = 1.4$.

value. Therefore, if shock forms at this location, the difference $\beta_i - y^*$ would be maximum. After M_1, the value of the integral $\int_0^y (f(M) - f(M_i))/f(M_i)\,\mathrm{d}y$ starts decreasing from its maximum value and eventually vanishes at a point M_2. Thus, although shock formation is favoured from M_1 to M_2 according to (4.9), the difference $\beta_i - y^*$ decreases. If shock forms at y_2 (corresponding to the Mach number M_2), y_2^* will be equal to β_i. After M_2, the condition (4.10) holds and shock formation is opposed.

The Mach number M_1 is one of the roots of the equation,

$$f(M) = f(M_i). \tag{4.17}$$

The plot M_1 versus M_i is shown in figure 5. It should be noted that the Mach number M_1 is independent of the base flow profile. If the Mach number profile of the base flow is known, the Mach number M_2 can be calculated from the relation,

$$\int_0^{y_2} \frac{(f(M) - f(M_i))}{f(M_i)}\,\mathrm{d}y = 0. \tag{4.18}$$

Case 2

Figure 3(c) depicts the case when M_i is greater than M_c. It is clear that $f(M_i)$ intersects the curve $f(M)$ only at one point M_i. Since $f(M)$ is always less than $f(M_i)$, the condition (4.10) holds, and consequently, shock formation is opposed.

Figure 6(a) depicts the evolution of the slope of the compressive disturbances in an accelerating flow. The Mach number profile considered here is exponential, i.e. $M(x) = \exp(\alpha x)$. The value of α is $1.0\,\mathrm{m}^{-1}$. The disturbance starts at Mach number 0.1 and propagates along the direction of flow. The value of the stagnation speed of sound a_{os} is chosen to be $500\,\mathrm{m\,s}^{-1}$. The value of γ is 1.4. Such a situation can be related to the disturbance propagating downstream in a rocket nozzle. The unsteady combustion process or a temporary partial blockage of the nozzle by slag in the case of a solid rocket motor may produce such disturbances. It can be seen from the figure that as the value of $|\sigma_i|$ is increased, the wave fronts become more and more unstable and after a critical value of $|\sigma_i|$, all the wave fronts eventually steepen into shock (the location of the shock is not shown in the figure).

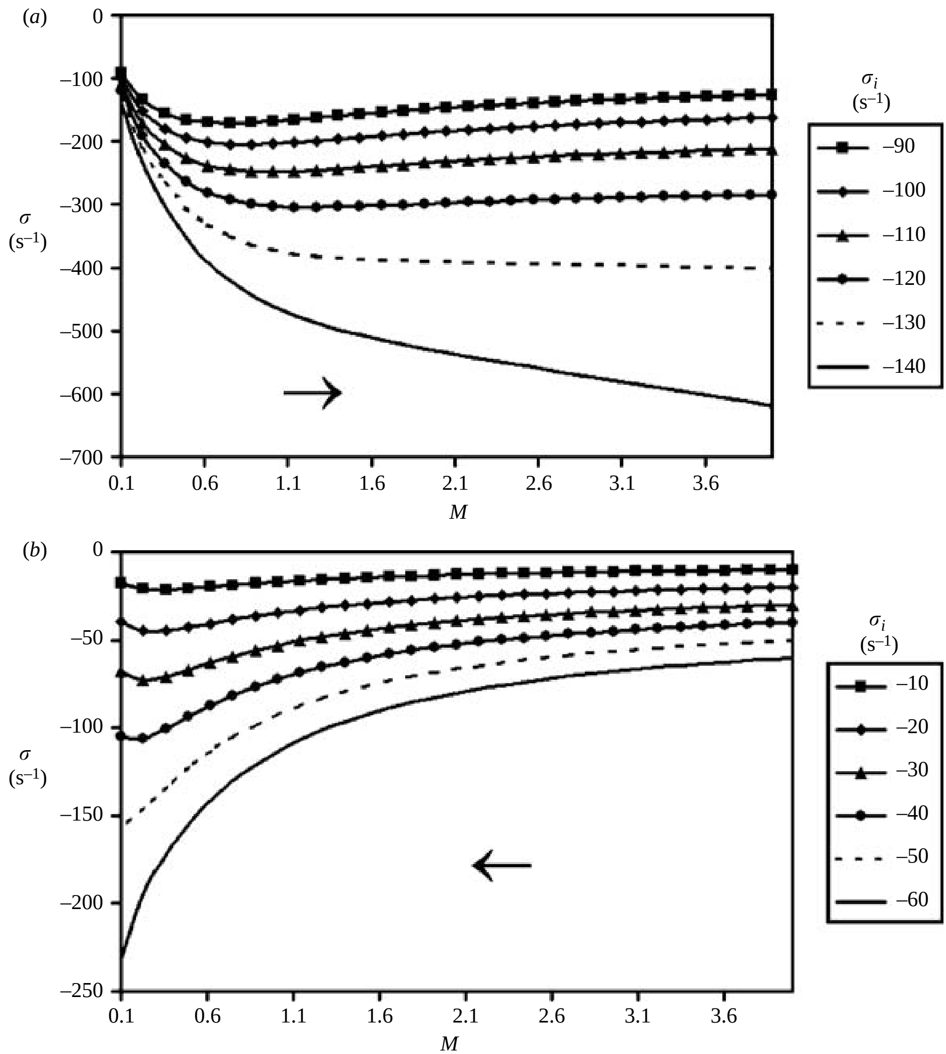

FIGURE 6. (*a*) The evolution of the slope of right-running compressive disturbances in an accelerating base flow. (*b*) The evolution of the slope of right-running disturbances in a decelerating base flow. The straight arrow on the figure shows the sense of temporal evolution.

4.1.2. *Decelerating flow*

In a decelerating flow in a C-D nozzle, the Mach number $M = M(x)$ is a decreasing function and thus has one-to-one correspondence with the distance x. Similar to the accelerating flow, we could use Mach number M as an independent variable instead of x. The same plot of $f(M)$ versus M as in §4.1.1 (figure 3*a*) can be used in the case of decelerating flow. However, in this case, the wave front moves from a higher Mach number to a lower Mach number, i.e. the wave front starting from Mach number M_i will find Mach number less than M_i. The situations when the wave front starts at Mach number $M_i > M_c$ (see figure3*b*) and when the wave front starts at Mach number $M_i < M_c$ (see figure 3*c*) are exactly the same as case 1 and case 2, respectively, in §4.1.1. For the decelerating flow, M_i should be read as M_1 in figure 5, and vice versa.

Figure 6(*b*) depicts the evolution of the slope of a compressive disturbance generated in an exponentially decelerating base flow. The values of α and a_{os} are $-1.0\,\mathrm{m}^{-1}$ and $500\,\mathrm{m\,s}^{-1}$, respectively. The disturbance starts at Mach number 4 and propagates along the flow. The value of γ is 1.4. This situation is similar to the propagation of disturbances in the intake of air-breathing engines (turbojet/ramjet/scramjet) moving at supersonic speed. The disturbances could be generated by a sudden variation in the speed of the vehicle or change in the ambient conditions. It can be seen from the figure that as the value of $|\sigma_i|$ is increased, the wave fronts become more and more unstable and after a critical value $|\sigma_i|$ all the wave fronts eventually steepen into shock. However, the values of $|\sigma_i|$ for which wave fronts steepen into shock are much less then that in the case of an accelerating flow (§ 4.1.1, figure 6*a*).

5. Nonlinear steepening of a left running wave

In this section, the nonlinear steepening of a left-running wave is investigated. For a left-running wave, the integrating factor $IF(y)$ (see (3.7)) is singular at $M=1$. Therefore, the analysis has to be performed separately in subsonic and supersonic flow, which is in agreement with the fact that a left-running wave front never crosses the unity Mach number.

In a subsonic flow, the velocity of the wave front $(u_0(y)-a_0(y))$ is negative and therefore the wave front will always be moving towards the negative x-axis. In this case, if it is assumed that a left-running wave front starts at $y=0$ and the subsonic base flow is extended up to $-\infty$ or up to the sonic point (yth), the condition of shock formation and the corresponding shock formation distance are:

$$|\sigma(0)| > \frac{IF(0)}{\displaystyle\int_0^{-\infty/y_{th}} IF(y)R(y)\,\mathrm{d}y}, \tag{5.1}$$

$$\int_0^{y^*} IF(y)R(y)\,\mathrm{d}y = \frac{IF(0)}{|\sigma(0)|}. \tag{5.2}$$

In the case of a supersonic base flow, the velocity of the wave front (u_0-a_0) is positive and the wave front will always be moving towards the positive x-axis. Similar to the subsonic base flow, consider a left-running wave starting at $y=0$ and the supersonic base flow is extended up to ∞ or up to the sonic point (y_{th}). Then the condition of shock formation and corresponding shock formation distance are given by (5.1) and (5.2), respectively, if $-\infty$ is replaced by $+\infty$ in (5.1).

5.1. *An example of flow in a converging–diverging* (*C-D*) *nozzle*

The base flow in the C-D nozzle is the same as described in § 4.1. Considering a left-running wave front starting at $x=x_i$ $(y=0)$ where the Mach number is M_i. The expression for the shock formation distance and the condition of shock formation are given by:

$$\int_0^{y^*} \frac{g(M)}{g(M_i)}\,\mathrm{d}y = \frac{2a_{0i}(M_i-1)}{(\gamma+1)|\sigma_i|} = \beta_i, \tag{5.3}$$

$$|\sigma_i| > \frac{2a_{0i}(M_i-1)}{(\gamma+1)\displaystyle\int_0^{\mp\infty/y_{th}} \frac{g(M)}{g(M_i)}\,\mathrm{d}y}, \tag{5.4}$$

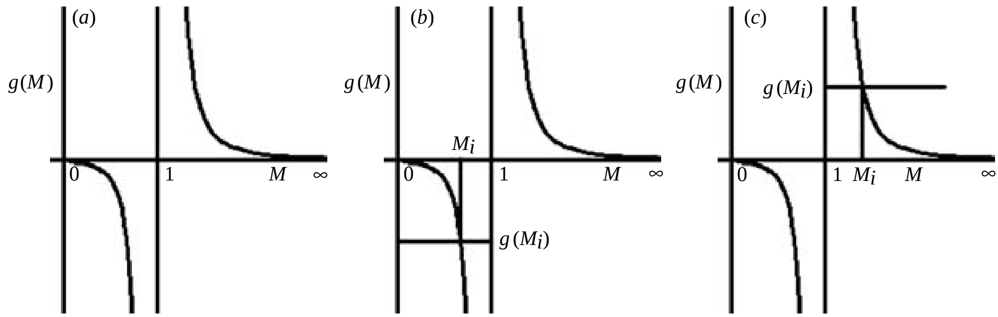

FIGURE 7. (*a*) Plot of $g(M)$ as function of M. It has singularity at sonic condition. (*b*) The case when the disturbance is created in subsonic flow. (*c*) The case when the disturbance is created in supersonic flow.

where the function $g(M)$ is:

$$g(M) = \frac{2\left(1+\frac{1}{2}(\gamma-1)M^2\right)\sqrt{M}}{(\gamma-1)(M-1)^3}. \tag{5.5}$$

In (5.4), in the upper limit of the integral, the negative sign is for subsonic flow and the positive sign is for supersonic flow. It should be noted that in decelerating flow, a left-running wave will move towards the sonic throat (§ 5.1.2), and therefore, the upper limit of integration in (5.4) will be y_{th} instead of $\pm\infty$. In the case of a left-running wave, β_i is:

$$\beta_i = \beta_s \frac{M_i - 1}{\sqrt{1+\frac{1}{2}(\gamma-1)M_i^2}}. \tag{5.6}$$

Similar to the right-running wave, the conditions favouring and opposing shock formation can easily be derived. Denote the integral $\int_0^{y^*} (g(M)-g(M_i))/g(M_i)\,\mathrm{d}y$ by G. Then, the conditions favouring shock formation will be:

$$G > 0 \text{ for supersonic flow and } G < 0 \text{ for subsonic flow,} \tag{5.7}$$

and the conditions opposing shock will be:

$$G < 0 \text{ for supersonic flow and } G > 0 \text{ for subsonic flow.} \tag{5.8}$$

5.1.1. *Accelerating flow*

The plot of $g(M)$ as a function of M is shown in figure 7(*a*) for $\gamma = 1.4$. This function is singular at $M = 1$. In subsonic flow, $g(M)$ is negative and monotonically decreases from 0 to $-\infty$. In supersonic flow, $g(M)$ is positive and monotonically decreases from ∞ to 0. It is clear that a wave front in either region will move away from the nozzle throat. We can easily show that in this case, the condition (5.8) is always satisfied (see figures 7*b* and 7*c*). Thus, in an accelerating flow, shock formation is always opposed for a left-running wave.

Figure 8 depicts the evolution of the slope of a left-running compressive disturbance propagating in an accelerating flow for subsonic and supersonic flow. The variation of Mach number is the same as that taken in § 4.1.1. The stagnation value of the speed of sound is 500 m s^{-1}. The value of γ is 1.4. In the subsonic flow, the disturbance starts at Mach number 0.8 and propagates against the flow. In the supersonic flow, disturbance starts at Mach number 1.2 and propagates along the flow. It can be seen from the figures that as the value of $|\sigma_i|$ is increased, the wave fronts become more and more unstable and after a critical value $|\sigma_i|$ all the wave fronts eventually steepen

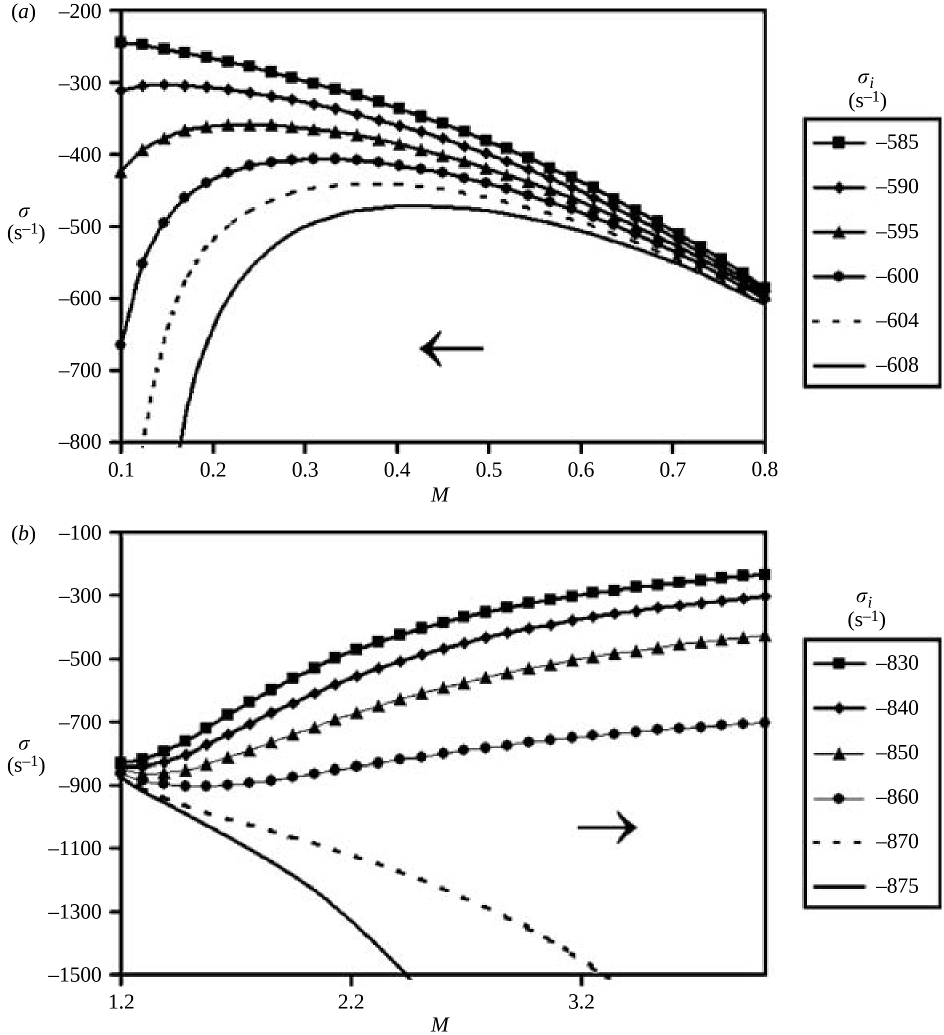

FIGURE 8. (*a*) The evolution of the slope of left-running compressive disturbances in the subsonic region of an accelerating base flow. (*b*) The evolution of the slope of left-running compressive disturbances in the supersonic region of an accelerating base flow. The straight arrow on the figure shows the sense of temporal evolution.

into shock. A comparison with figure 6 reveals that the order of magnitude of $|\sigma_i|$ at which steepening takes place for left-running waves is much higher than that for right-running waves.

5.1.2. *Decelerating flow*

In a decelerating flow, a left-running wave front in either region will move towards the throat of the nozzle. It can easily be shown that the condition (5.7) is always satisfied (see figure 7*b*, *c*). Thus, in decelerating flow, shock formation is favoured for the left-running compressive wave. As the left-running wave front moves towards the throat, the magnitude of its velocity $(u_0 - a_0)$ keeps on decreasing and becomes zero at the throat. As a consequence of this, if a wave front does not steepen into a shock, it will take infinite time to reach the throat (a rigorous proof is possible using the properties of indefinite integrals). However, a compressive wave front will evolve into a shock before reaching the throat (see Appendix A for the proof). Therefore, only an expansion wave front can approach the throat without evolving into a shock.

In this particular case, it will be interesting to see the behaviour of an expansion wave front as it approaches the throat. The slope of the expansive disturbance at the throat is given by (see Appendix B for the derivation):

$$\sigma_{th} = \lim_{\substack{y \to y_{th} \\ x \to 0}} \sigma = \frac{-4\sqrt{2}a_{0s}[\mathrm{d}M(x)/\mathrm{d}x]_{x=0}}{(\gamma+1)^{3/2}}. \tag{5.9}$$

Using (4.3), we can show that:

$$M'(0) = -\sqrt{(\gamma+1)/4}\sqrt{A''(0)/A(0)}. \tag{5.10}$$

Substituting this into (5.9) yields:

$$\sigma_{th} = 2\sqrt{2}a_{os}\sqrt{A''(0)/A(0)}/(\gamma+1). \tag{5.11}$$

This is the limiting value of the slope of the disturbance as it approaches the nozzle throat. It is interesting to note that σ_{th} is independent of the initial slope of the wave front. Therefore, at the throat, an expansion wave front having an initial slope σ_i greater than σ_{th} will relax by an amount $\sigma_i - \sigma_{th}$ and an expansion wave front having initial slope less than σ_{th} will steepen by an amount $\sigma_{th} - \sigma_i$. Thus, all the left-running expansion waves in a decelerating flow in a choked C-D nozzle always tend towards a fixed strength disturbance. Such expansion waves are called quenching waves. Clarke (1977) showed the existence of similar quenching waves in a chemically reacting media. The strength (σ_{th}) of these expansion waves at the nozzle throat depends upon the geometry of the nozzle at the throat.

Figure 9 depicts the evolution of expansive disturbances in subsonic and supersonic base flows. The decelerating base flow is the same as in §4.1.2. In the subsonic region, the disturbance starts at Mach number 0.1 and propagates along the base flow towards the nozzle throat. In the supersonic region, the disturbance starts at Mach number 4 and propagates across the base flow towards the nozzle throat. It can be seen that in both cases, the slopes of all the expansive disturbances created in either regions approach the same finite value of $760.726\,\mathrm{s}^{-1}$. Such a high value shows that the expansion wave front near the throat will be steep.

Table 1 summarizes the different cases discussed in §4 and §5.

6. Conclusions

The nonlinear steepening of disturbances in a steady non-uniform homentropic flow is studied using the method of characteristics. It is found that only compressive disturbances can cause shock formation in such flows. An expression for the minimum value of the slope of the disturbance in order for a disturbance to steepen into a shock is obtained. An implicit relation for the location of shock formation is also obtained. Shock formation in a choked converging–diverging (C-D) nozzle is analysed for both right-running and left-running waves.

The nonlinear analysis performed in the paper has the following distinct advantages over a linear analysis. Linear stability analysis assumes that the initial disturbance is small and predicts only the initial behaviour of disturbance, i.e. whether it will grow or decay. On the other hand, the nonlinear analysis performed in the present paper

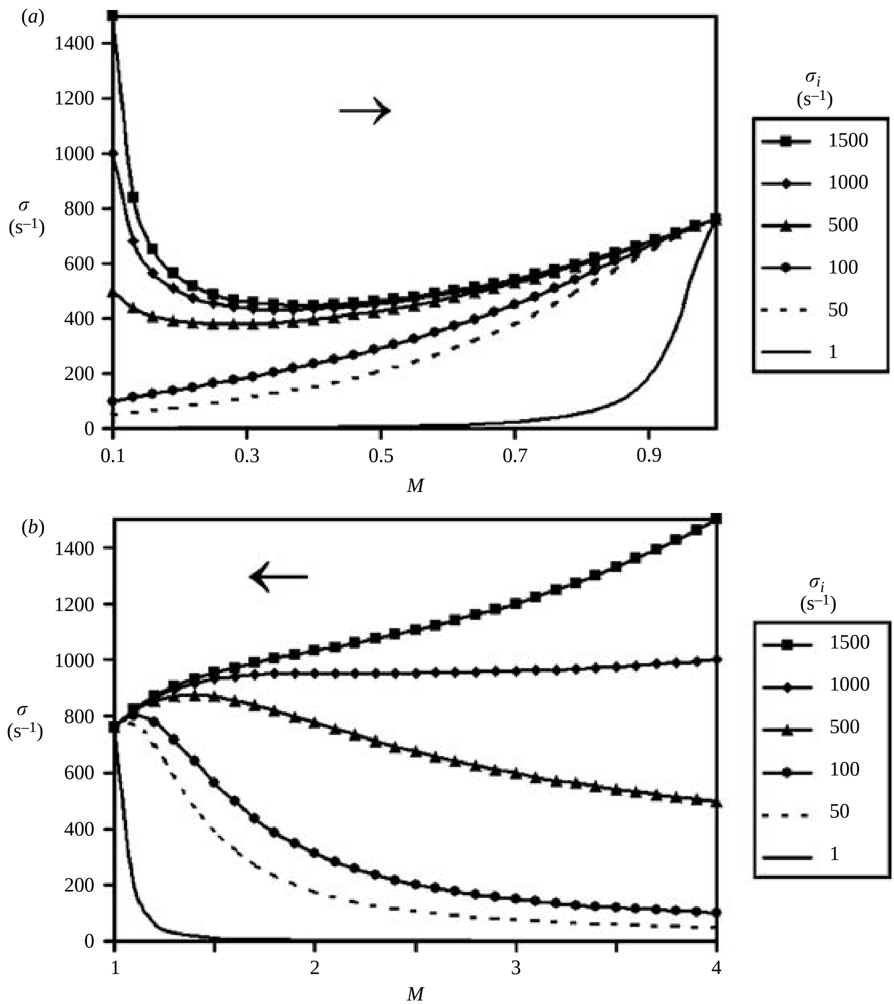

FIGURE 9. (a) The evolution of the slope of left-running expansive disturbances in the subsonic region of a decelerating base flow. (b) The evolution of the slope of left-running expansive disturbances the supersonic region of a decelerating base flow. The straight arrow on the figure shows the sense of temporal evolution.

Right-running wave		
Accelerating flow	Location of initial disturbance	Tendency of shock formation
	$M_i < M_c$	Favoured if $M_s < M_2$
		Opposed if $M_s > M_2$
	$M_i > M_c$	Opposed
Decelerating flow	$M_i < M_c$	Opposed
	$M_i > M_c$	Favoured if $M_s < M_2$
		Opposed if $M_s > M_2$
Left-running wave		
Accelerating flow		Opposed
Decelerating flow		Favoured

TABLE 1. The tendency of a compressive disturbance to steepen into shock in various flow situations considered in the paper. The notation is the same as that used in the text. Here, M_s is the Mach number of the base flow corresponding to the location where shock forms.

gives the long time behaviour of a disturbance of arbitrary strength (initial slope), and gives the location of shock if it forms, which is not possible using the linear stability analysis. Furthermore, the linear stability analysis is independent of the initial strength of the disturbance. However, the present paper demonstrates that the initial strength of the disturbance is very important. In many cases, shock formation is possible only if the initial strength of a compressive disturbance exceeds a minimum value.

The important findings of the present paper are:

1. In the case of right-running waves, there exists a critical Mach number whose value is around 0.208. In an accelerating flow in a C-D nozzle, if the wave starts at a Mach number greater than this critical Mach number, shock formation is always opposed. However, if the wave starts at a Mach number less than this critical Mach number, shock formation may or may not be opposed, depending upon where the shock forms. In decelerating flow, if the wave starts at a Mach number less than the critical Mach number, shock formation is opposed, and if it starts at a Mach number greater than the critical Mach number, shock formation may or may not be opposed, depending upon where the shock forms.

2. In the case of a right-running wave in an exponentially accelerating or decelerating flow, shock forms only if the initial slope of the compression wave front exceeds a minimum value.

3. In the case of left-running waves, shock formation is always opposed if the base flow in the C-D nozzle is accelerating. On the other hand, if base flow is decelerating, shock formation is favoured, and a compression wave will blow up before reaching the throat.

4. In the case of a left-running wave in an exponentially accelerating flow, shock forms only if the initial slope of the compression wave front exceeds a minimum value.

5. Left-running expansion waves tend towards a permanent form in decelerating flow in a C-D nozzle.

In the end, a comment about the stability of base flow, particularly in the transonic region, towards a gasdynamic disturbance seems to be necessary. It is clear from table 1 that in the case of accelerating base flow, if a compressive disturbance is produced near the throat (in the transonic region), shock formation is opposed for both right- and left-running waves. On the other hand (in the transonic region), in a decelerating base flow, shock formation is favoured. Thus, in view of the explanation given in § 1, accelerating flow is comparatively more inertially stable compared to decelerating flow in transonic region, which is consistent with the findings in the existing literature.

This work was funded by Indian Space Research Organization (ISRO). The authors thank Dr V. Ramamurthi, Liquid Propulsion Systems Center, ISRO for his interest in this work. The authors further wish to thank Dr S. R. Chakravarthy and Mr P. Bala Subrahmanyam, IIT Madras for their comments and suggestions during different stages of this work. Thanks are also due to an anonymous referee for finding the exact explicit solution of (4.12).

Appendix A

For a left-running wave front in a decelerating flow, the condition of shock formation will be (5.4):

$$|\sigma_i| > 2a_{0i}(M_i - 1) \bigg/ \left((\gamma + 1)\int_0^{y_{th}} g(M)/g(M_i)\,\mathrm{d}y\right). \tag{A 1}$$

Here, $y_{th}=y_{th-}$ in subsonic flow and $y_{th}=y_{th+}$ in supersonic flow. Consider the following integral:

$$\int_0^{y_{th-}} g(M)\,\mathrm{d}y = \int_{x_i}^{x_{th-}} g(M)\,\mathrm{d}x = \int_{M_i}^{1-} \frac{g(M)\,\mathrm{d}M}{M'(x)}. \tag{A 2}$$

Let the maximum value of $|M'(x)|$ be Γ_1 on $[M_i, 1]$. Then

$$\left|\int_{M_i}^{1-} \frac{g(M)\,\mathrm{d}M}{M'(x)}\right| \geqslant \left|\Gamma_1 \int_{M_i}^{1-} g(M)\,\mathrm{d}M\right|. \tag{A 3}$$

Now using (5.11),

$$\int_{M_i}^{1-} g(M)\,\mathrm{d}M = \lim_{M\to 1-} \int_{M_i}^{M} g(M)\,\mathrm{d}M = \lim_{M\to 1-} [F(M) - F(M_i)] = -\infty. \tag{A 4}$$

Thus, the integral $\int_0^{y_{th-}} g(M)\,\mathrm{d}y$ is divergent. In a very similar fashion, we can show that the integral $\int_0^{y_{th+}} g(M)\,\mathrm{d}y$ is also divergent. Therefore, the condition (A 1) will always be satisfied, and hence every left-running compression wave moving towards the sonic throat will eventually evolve into a shock before reaching the throat.

Appendix B

The slope of a left-running expansion wave front as it approaches the throat can be calculated by taking the limit as $y \to y_{th}$ or $M \to 1$ in (3.3). Consider a left-running expansion wave front moving in subsonic flow approaching the sonic throat. Then,

$$\begin{aligned}
\lim_{\substack{y\to y_{th-}\\ M\to 1-}} \frac{1}{\sigma} = {} & \lim_{\substack{y\to y_{th-}\\ M\to 1-}} \left[\left(\frac{a_0(0)\left(1+((\gamma-1)/2)M_i^2\right)\sqrt{M_i}}{(M_i-1)^2}\right)\right. \\
& \times \left.\left(\frac{(M-1)^2}{a_0(y)(1+((\gamma-1)/2)M^2)\sqrt{M}}\right)\right] \\
& + \lim_{\substack{y\to y_{th-}\\ M\to 1-}} \left[\left(\frac{(\gamma+1)(M-1)^2}{2a_0(y)(1+((\gamma-1)/2)M^2)\sqrt{M}}\right)\right. \\
& \times \left.\left(\int_0^y \frac{(1+((\gamma-1)/2)M^2)\sqrt{M}}{(M-1)^3}\,\mathrm{d}y\right)\right].
\end{aligned} \tag{B 1}$$

The first limit on right-hand side is zero. To evaluate the second limit, change the variable of integration from y space to x space and then further to M space,

$$\lim_{\substack{y\to y_{th-}\\ M\to 1-}} \frac{1}{\sigma} = \lim_{\substack{y\to y_{th-}\\ M\to 1-}} \frac{\left(\displaystyle\int_{M_i}^{M} \frac{(1+((\gamma-1)/2)M^2)\sqrt{M}}{(M-1)^3 M'}\,\mathrm{d}M\right)}{1\Bigg/\left(\dfrac{(\gamma+1)(M-1)^2}{2a_0(x_{th})(1+((\gamma-1)/2)M^2)\sqrt{M}}\right)}. \tag{B 2}$$

Since the integral in the numerator is divergent (see Appendix A), the above limit is of the form ∞/∞. Applying L'Hopital's rule to evaluate the limit, we obtain,

$$\frac{1}{\sigma_{th-}} = \lim_{\substack{y \to y_{th-} \\ M \to 1-}} \frac{1}{\sigma} = \frac{-(\gamma+1)}{4M'(x_{th})a_0(x_{th})}. \tag{B 3}$$

In a similar fashion, we can show that

$$\frac{1}{\sigma_{th+}} = \lim_{\substack{y \to y_{th+} \\ M \to 1+}} \frac{1}{\sigma} = \frac{-(\gamma+1)}{4M'(x_{th})a_0(x_{th})}. \tag{B 4}$$

REFERENCES

Bhatnagar, P. L. & Prasad, P. 1971 Study of self-similar and steady flows near singularities Part 2: a case of multiple characteristics velocity. *Proc. R. Soc. Lond.* A **322**, 45–62.

Clarke, J. F. 1977 Chemical amplification at the wave head of a finite amplitude gasdynamic disturbance. *J. Fluid Mech.* **81**, 257–264.

Courant, R. & Friedrichs, K. O. 1948 *Supersonic Flow and Shock Waves*. Interscience.

Davis, H. T. 1962 *Introduction to Nonlinear Differential and Integral Equations*. Dover.

John, J. E. A. 1984 *Gas Dynamics*. Prentice-Hall, New Jersey.

Kantrowitz, A. R. 1947 The formation and stability of normal shock waves in channel flow. National Advisory Committee for Aeronautics, USA *Tech. Note* 1225. (available at http://naca.larc.nasa.gov).

Kulikovskii, A. G. & Slobodkina, F. A. 1967 Equilibrium of arbitrary steady flows at transonic points. *J. Appl. Math. Mech. Prikl. Math. Mech.* **21**, 623–30.

Kuo, Y. H. 1951 On the stability of two-dimensional smooth transonic flows. *J. Aero. Sci.* **18**, 1.

Liepmann, H. W. & Roshko, A. 1957 *Elements of Gasdynamics*. Willey.

Lighthill, J. 1978 *Waves in Fluids*. Cambridge University Press.

Lin, H. & Szeri, A. J. 2001 Shock formation in the presence of entropy gradients. *J. Fluid Mech.* **431**, 161–188.

Prasad, P. 1972 Non-linear approximation of a hyperbolic system in the neighborhood of a bicharacteristic curve and stability of two-dimensional and axi-symmetric steady transonic flows. *J. Math. Phys. Sci.* **6**, 89–112.

Prasad, P. 1973 Nonlinear wave propagation on an arbitrary steady transonic flow. *J. Fluid Mech.* **57**, 721–737.

Prasad, P. 2001 *Nonlinear Hyperbolic Waves in Multi-Dimensions*, pp. 173–204. Chapman & Hall/CRC.

Prasad, P. & Krishnan, E. V. 1977 Nonlinear wave propagation in a two-dimensional steady transonic flow. *J. Fluid Mech.* **82**, 17–28.

Thompson, P. A. 1972 *Compressible Fluid Dynamics*, pp. 198–201. McGraw-Hill.

Tyagi, M. & Sujith, R. I. 2003 Nonlinear distortion of travelling waves in variable area ducts with entropy gradients. *J. Fluid Mech.* **492**, 1–22.

Whitham, G. B. 1974 *Linear and Nonlinear Waves*. Wiley.